Water Practice & Technology

IWA PUBLISHING

Water Practice & Technology Vol 18 No 6, 1576 doi: 10.2166/wpt.2023.079

Impacts of climate and land use/cover change on mini-hydropower generation in River Kyambura watershed in South Western part of Uganda

Musa Aruho Tusingwiire, Martin D. Tumutungire, Jotham Ivan Sempewo* and Swaib Semiyaga

Department of Civil and Environmental Engineering, Makerere University, Kampala, Uganda
*Corresponding author. E-mail: jothamsempewo@yahoo.com; jotham.sempewo@mak.ac.ug

JIS, 0000-0002-9897-211X

ABSTRACT

This study explored the combined impacts of climate and land-use change on mini-hydropower generation in the Kyambura watershed. The soil and water assessment tool (SWAT) was used as a hydrological model whereas the statistical downscaling model (SDSM) was used to downscale meteorological data for the Kyambura watershed for the year 2050. The results show that there will be an increase in urban land by 11.89%, barren land by 25.78%, water by 0.49% and a reduction in percentage area coverage of vegetation by 38.17% by the year 2050. A 10.6 and 17.7% increase is anticipated in average annual hydropower generated by the year 2050. There is, therefore, a need to develop governing policies to regulate management practices to preserve the integrity of the watersheds and ensure the reliability of power production.

Key words: ArcSWAT, climate change, hydropower, land-use/cover change

HIGHLIGHTS

- Quantifies LULC changes within the Kyambura catchment from 1989 to 2019.
- Predicts and quantifies LULC changes within the Kyambura catchment by the year 2050.
- Predicts the changes in climate, stream flows and Hydropower generation within the Kyambura catchment by the year 2050.
- Elucidates on the impacts of climate and Land use/cover change on mini-hydropower generation.

GRAPHICAL ABSTRACT

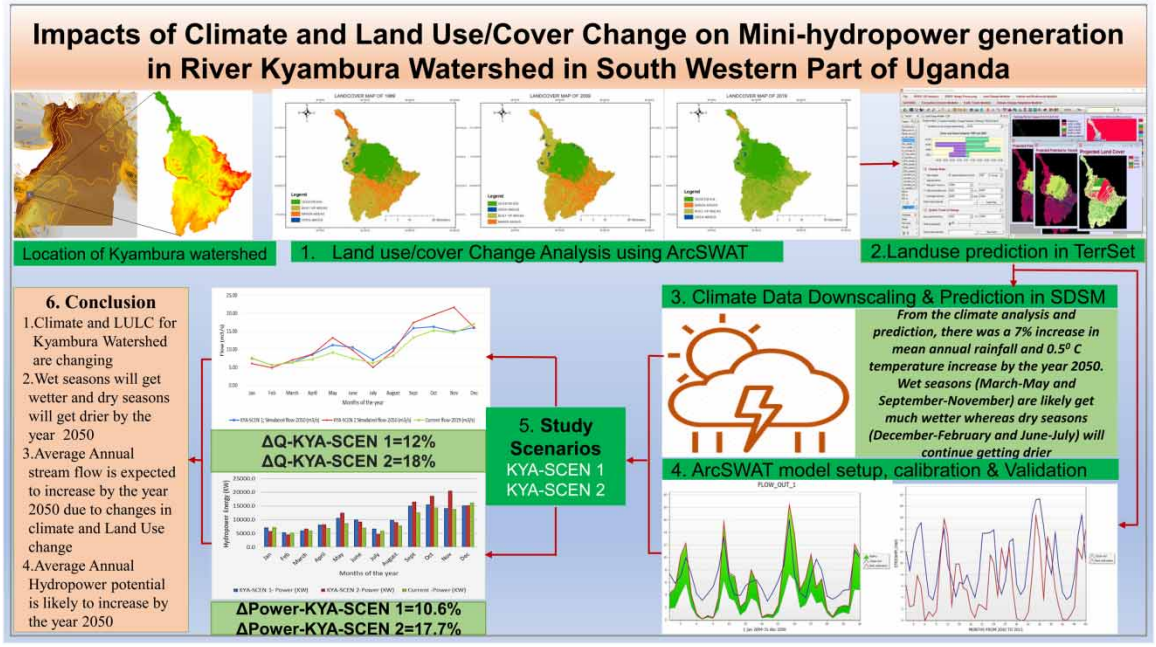

1. INTRODUCTION

The world's environmental challenge today is climate change (Pachauri *et al.* 2014). Climate change is defined as an alteration of climate, accountable definitely or indefinitely to anthropogenic activities, that changes the structure of the global atmosphere and is discerned over a time period, distinguishing it from the natural climate instability (Houghton *et al.* 2001). The fifth climate change assessment report (Pachauri & Meyer 2014) of the United Nations Intergovernmental Panel on Climate Change (IPCC) states that there has been an increase in the average global Bu *et al.* 2014 surface temperature in the twenty-first century due to increasing cumulative greenhouse gas emissions such as CO_2. Rising temperatures accelerate the hydrological cycle through enhanced evaporation. Additionally, the intensity, frequency and spatial distribution of precipitation have continuously changed (Labat *et al.* 2004). Rising temperatures and changes in precipitation have a significant impact on water resources in a river basin (Fengping *et al.* 2013).

Complex spatio-temporal hydrological processes influence water distribution within a watershed (Melih Ozturk 2013). These are in turn related to numerous meteorological, surface and sub-surface characteristics. Changes in land use and land cover (LULC) are one of the main human-induced activities altering the hydrological system (Calder 1998). Land use and land cover change (LULCC) seriously affect water resources (Memarian *et al.* 2013). Land use/cover change is the most direct interaction that links human activities and natural ecological processes (Liu *et al.* 2014). Land use/cover changes directly affect the condition of water resources and agricultural economic growth (Bu *et al.* 2014).

Changes in both climate and land use/cover have an effect on water resources. Many studies on assessing the effect of land use change on streamflow have been done on a global scale (Amini *et al.* 2011; Bosmans *et al.* 2016; Welde & Gebremariam 2017; Guzha *et al.* 2018) and climate change on river flows (Ogiramoi 2011; Taylor *et al.* 2014; Taye *et al.* 2015; Duong *et al.* 2016; Kangume 2016). To mitigate climate change impacts, several solutions have been proposed to reduce greenhouse gas emissions. These include better human practices (land use/cover practices) such as afforestation, modern efficient energy alternatives and enhancing the use of sustainable energy sources. Hydropower has a significant role to play in the era of climate change where green energy is the key to reducing global warming (Bartle 2002). Hydropower is so far the most lucrative option due to its renewability, lower emissions and longevity of infrastructure (Li *et al.* 2018). Though the hydropower sector makes a significant effort to cope with today's rising world energy demands, this is difficult due to climate and land use/cover change effects. Madani (2011) stated that climate change will have a variety of effects on streamflow, involving quantity and timing, sediment load, temperature and ecosystem changes. Temperature fluctuations, rainfall patterns, floods and droughts are all major signs of climate change that have strong effects on river systems, which will consequently affect hydropower generation. Changes in land use/cover impact the stream flows of a river (Musa & Eliot 2018). The decreasing ability of the catchment to retain water for a reasonable period of time results in a fluctuating river flow mostly during dry spells. The possible recession of river flow may lead to decreased hydropower generation. According to Cole *et al.* (2014) in Kenya, a drought over the period 1998–2000 reduced hydropower production due to decreased streamflow, while in Ghana in 1998 shortages in rainfall caused hydropower production to fall by up to 40%. In both 2006 and 2011, Tanzania experienced energy crises due to droughts. These examples give an insight into how climate variability together with uncontrolled land use and land cover changes could impact hydropower potential.

In Uganda, such trends have been experienced in several watersheds such as the river Mpanga watershed. The flow of river Mpanga has been dwindling with time. This has negatively affected the hydropower production capacity of the Mpanga mini-hydropower station to an extent that it is sometimes shut down due to low power generation (Taylor *et al.* 2015). The installed capacity of 18 MW has since been reduced to 12 MW. According to Saem Engineering Company Limited, which that is currently running the hydropower project, human degradation within the river catchment is heavily affecting power generation at the Mpanga hydropower station. Human activities along the river banks such as poor agricultural practices, encroachment, pollution, and sand and stone extraction among others have resulted in silting, reduction in water levels and reduced water flow. These have in turn led to a reduction in power generation (Amanyire 2019).

Electricity is very important for national development. In Uganda, greater electricity generation is needed to compensate for the ongoing population growth and the emerging industries and factories (Taylor *et al.* 2015). The country is under pressure to find additional energy sources, as electricity demand is growing at an annual rate of 10–12% (Kees & Stephen 2018). Medium and small new hydropower plants are being constructed and

some have been completed to meet the country's rising demand for electric energy. Uganda has embarked on a drive to increase its hydropower production which is mainly generated from the 255 MW Bujagali, the 200 MW Kiira and 180 MW Nalubaale plants by developing new hydropower plants (Rugumayo *et al.* 2014). The government has a major expansion plan to double generation, from 2.5 TWh in 2010 to around 5 TWh by 2030, from the development of both large, medium and small hydropower. Among the small hydropower plants is the 7.6 MW capacity Kyambura station, which is a runoff-river station that is fed by River Kyambura (Renewgen 2021).

In this regard, many studies have been carried out on both global and regional levels; assessing the impacts of climate change on hydropower generation (Hamududu & Killingtveit 2012; Gaudard *et al.* 2013, 2014) and land use changes on hydropower generation (Tilak 2010; Khare *et al.* 2017; Serrão *et al.* 2020). However, most of the researchers have focused on either the effects of climate change or land use change on hydropower generation at global and regional levels. Little research has been done on individual river catchments. Furthermore, even among research carried out on a catchment level, very few such as Bahati *et al.* (2021) have studied the coupled effects of changes in both land use and climate on either streamflow or hydropower. A study was done on the Muzizi hydropower plant in Uganda by Bahati *et al.* (2021). In this study, a climate model in a data-scarce scenario was built using bias-corrected reanalysis data and historical discharge data to evaluate the potential impacts of land use and climate change on hydropower reliability. Neema (2018) carried out a study into the effect of climate change on river flow in the Kyambura catchment. However, even with the establishment of the small hydropower station, research on the coupled effects of changes in land use/cover and climate on the Kyambura mini-hydropower station within the catchment have not been carried out. Furthermore, different catchments have different characteristics and hydrologically behave or respond differently. It may, therefore, not be applicable to make the same or similar conclusions for the Kyambura catchment based on studies done on other catchments.

This study aimed at modeling the impacts of climate and land use/cover change on mini-hydropower generation in the River Kyambura watershed in South-Western part of Uganda. To assess the possible impact of changes in both climate and land use/cover on hydropower generation, analysis of the river flow related to the climate and land use variability is required, as it will help planners and managers operate the hydropower plant efficiently as well as help in developing decision support systems to maintain the integrity of river Kyambura.

In this study, the SWAT, Land Change Modeler (LCM) of the TerrSet Geospatial Monitoring and Modeling system Software and a Statistical DownScaling Model (SDSM version 4.2) were used. SWAT, which is basically a river basin model was used to simulate river flow. The SWAT model is a physically based semi-distributed hydrologic model operating on a daily time step. It is a river basin, scale model developed to forecast the impact of land management practices on water, sediment and agricultural chemical yields in conditions over long periods of time (Winchell *et al.* 2010). The model uses physical algorithms to estimate runoff. Using data such as precipitation, soil properties, topography, land cover and management account, the model calculates the runoff using the SCS curve number equation (Abbaspour 2007). The inputs of the SWAT model are readily available. It is efficient and enables users to study long-term impacts. Land-use Change Modeler (LCM) of TerrSet was used for Land Use change prediction and the SDSM was used to downscale the daily timestep precipitation and temperature data. It was also used to predict future climatic conditions (temperature and precipitation) for the year 2050.

The ArcSWAT ArcGIS extension is a graphical user interface for the SWAT model (Arnold *et al.* 1998). This interface is user friendly since it is embedded in ArcGIS, a necessary tool for studies where the SWAT model is applicable. The ArcSWAT ArcGIS extension evolved from AVSWAT2000, an ArcView extension developed for an earlier version of SWAT (Di Luzio 2001). The interface requires the designation of land use, soil, weather, groundwater, water use, management, soil chemistry, a pond and stream water quality data, as well as the simulation period, in order to ensure a successful simulation (Winchell 2010). The hydrologic simulation of SWAT is based on the following water balance equation (Neitsch *et al.* 2011):

$$SW_t = SW_0 + t_{i=1}(R_{day} - Q_{surf} - E_a - W_{seep} - Q_{gw}) \quad (1)$$

where SW_t is the final soil water content (mm), SW_0 is the initial soil water content on day i (mm), t is the time (days), R_{day} is the amount of precipitation on day i (mm), Q_{surf} is the amount of surface runoff on day i (mm), E_a is

the amount of evapotranspiration on day i (mm), W_{seep} is the amount of water entering the vadose zone from the soil profile on day i (mm) and Q_{gw} is the amount of return flow on day i (mm).

General circulation models (GCMs) are restricted by their coarse spatial resolution in their usefulness for local impact studies. They also cannot resolve useful sub-grid scale features such as topography and clouds (Wilby *et al.* 2002). In this study, a low-cost, rapid assessment of highly localized climate change impacts was required. Therefore, statistical downscaling was chosen over dynamic downscaling. Under current and future regional climate conditions, SDSM facilitates the rapid development of multiple, low-cost, single-site scenarios of daily surface weather variables. Additionally, the software performs ancillary tasks of predictor variable pre-screening, model calibration, basic diagnostic testing, statistical analyses and graphing of climate data (Wilby & Dawson 2007).

TerrSet is a geospatial and monitoring software that incorporates the IDRIS GIS and Image Processing tools (Ronald Eastman 2016). It offers a constellation of vertical applications focused on monitoring and modeling earth systems; among which is the LCM. The LCM incorporates a CA-Moakov chain-based neural network to predict future LULC (Sundara Kumar *et al.* 2015). The LCM was found to be very effective during this study.

In this paper, data for the Kyambura basin, including meteorological data, streamflow data, elevation, hydrology, slope, land use, soil type and land-cover maps, were used. SDSM software was used to downscale meteorological data and perform climate predictions of the Kyambura Catchment for the year 2050. The different land use images were classified into four major land use types (Built-up land, Vegetation, Barren land and Open water) using ArcMap 10.5. The Land Change Management (LCM) of TerrSet software was used to perform predictions of the possible land use changes by the year 2050. The SWAT model was employed to assess the effects of changes in land use types on water resources considering climate change in the Kyambura catchment. The results can help water conservancy administrative departments in land use planning and water resource management.

2. STUDY AREA

The study was carried out in the catchment of river Kyambura, which is about 4,000 km^2 and stretches across Buwheju, Bushenyi, Rubirizi and Kasese districts in the south-western part of Uganda. The river is 25 km long and flows north-west from the Kasyoha-Kitomi forest in the hills of Buwheju, draining into the Kazinga channel. Figure 1 shows the location of the study area on the map of Uganda.

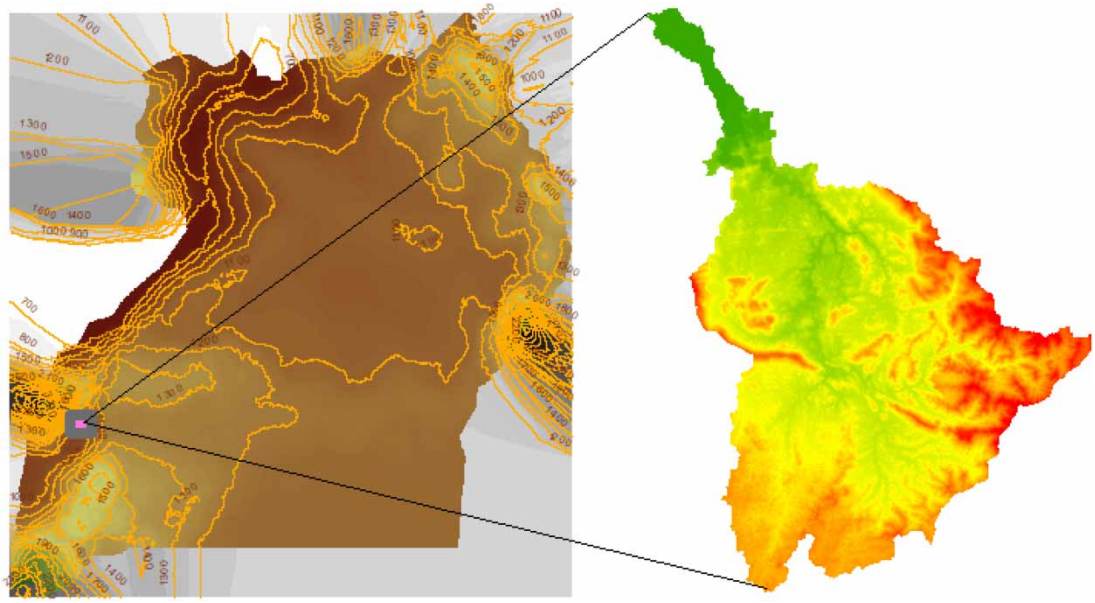

Figure 1 | The location of the River Kyambura catchment on the map of Uganda.

The total population of the four districts that make up the Kyambura catchment is about 1,179,301 people which is 3.38% of the 34.9 million people in Uganda (UBOS 2016). There are 39 sub-counties and 228 parishes in the Kyambura catchment. The highest number of people in this area are farmers. Crops such as cotton, coffee, millet, bananas and maize, among others, are mostly grown in the region. Cattle keeping is yet another economic

activity that a few of the people in this area participate in. In Kasese and Rubirizi, tourism is a key source of revenue and income for the locals due to the many tourists that traverse this particular area for wildlife touring in the Kyambura game reserve and Queen Elizabeth national park.

The Kyambura mini-hydropower station is geographically located at coordinates: 00°12′39.0″S, 30°07′04.0″E (Latitude:-0.210833; Longitude:30.117778), in the Kyambura area, across the Kyambura River, in Kiruggu subcounty, Rubirizi District, approximately 10.5 km, north of the town of Rubirizi. The station which was tested to the national grid in July 2019 and commenced commercial output in August 2019, is a runoff-river installation with a generation capacity of 7.6 MW (10,200 hp) and annual production of 36.7 GWh. The design flow is 5 m^3/s with a gross head of 102 m (Renewgen 2021).

There are several land use and land cover changes that have occurred and are still occurring within the Kyambura catchment which if not controlled, may impose severe consequences on the river catchment water yield. These include but are not limited to deforestation to obtain wood for charcoal burning and timber, conversion of large areas to agricultural land to meet the increasing demand for raw materials for the growing factories such as cotton ginneries, and tea factories among others as well as the increasing demand for food due to the rising population. The built-up area has increased in the catchment due to urbanization.

3. MATERIALS AND METHODS

3.1. Materials and software

In this study, ArcSWAT, an ArcGIS/ArcMap extension was used. SWAT is a distributed hydrological model which has been used widely by researchers for various studies. The SWAT model is globally used because it is open sourced, it has high computational efficiency, the input variables can be easily obtained, it provides long-term watershed simulation and it can be modified based on the actual characteristics of any watershed. The SDSM software was used to downscale meteorological data and project changes in mean temperatures and rainfall/climate of the Kyambura watershed for the year 2050. Land use images were processed and classified using ArcMap 10.5. TerrSet software was used to project land-use changes within the catchment by the year 2050.

Spatial, meteorological, soil, daily river flow and land use/cover data were prerequisites for developing the SWAT model for the Kyambura catchment. The daily time series of hydro-meteorological data of the Rubirizi-saza-quarter weather station for a 31-year period (1989–2019) was obtained from the NASA website. STRM DEM with 30 m resolution which was used to delineate the catchment, was downloaded from Earth Explorer on the United States Geographic Survey (USGS) website. River flow data for the Kyambura gauging station located at lat. 00°11′22″S, lon. 030°06′11″E besides the Kyambura-Katerera bridge were obtained from the Directorate of Water Resource Management (DWRM). The land use data were obtained from the land cover grid maps which were generated using supervised classification of Landsat Images. Distance from the river, roads and urban area maps which were prerequisite variables for the land cover prediction in TerrSet were generated using the ArcGIS tools of ArcMap 10.5.

3.2. Stream flow and meteorological data analysis

The meteorological and river flow data were tested for consistency, trend and randomness. Figures 2–4 show the trend of average annual precipitation, temperature and river Kyambura stream flow, respectively, for the period of 1989–2019. From the figures, it is evident that there has been generally positive trend in precipitation, temperature and stream flows. Average annual precipitation increased by 3.8 and 10.0% for periods (1989–2009) and (2009–2019), respectively. Average annual temperatures generally increased by 42.6% for the period (1989–2009) and decreased by 1.0% for the period (2009–2019). Average annual stream flows reduced by 1.2% for the period of (1989–2009) and increased by 5.0% for the period (2009–2019) as shown in Table 1.

Figure 5 shows the variability between precipitation and Kyambura stream flows. Flows were averagely normal for the period from 1989 to 2003. Between 2003 and 2015, flows generally dwindled even with heavy rainfall.

3.3. Land use/cover change analysis

Landsat 5, 7 and 8 data were obtained for the years 1989, 2009 and 2019. Image enhancement was done to modify the image values aimed at improving the visual interpretability of an image. Some of the enhancement procedures used include haze reduction and destripping. The identification of land cover classes in the images was done with reference to the Food and Agriculture Organization (FAO) Afri-cover land classification system. A supervised land cover classification was done by; selecting training samples for each of the

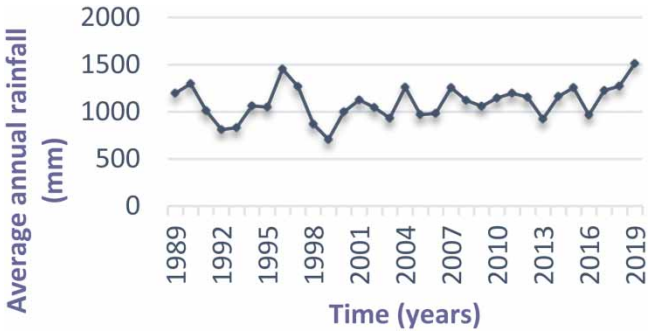

Figure 2 | The average annual rainfall trend for a period from 1989 to 2019.

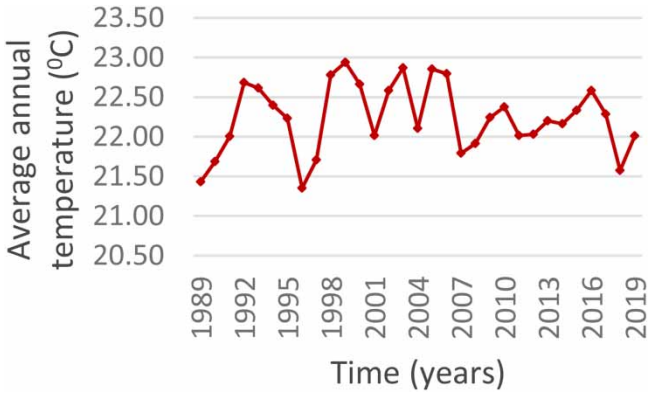

Figure 3 | The average annual temperature trend for a period from 1989 to 2019.

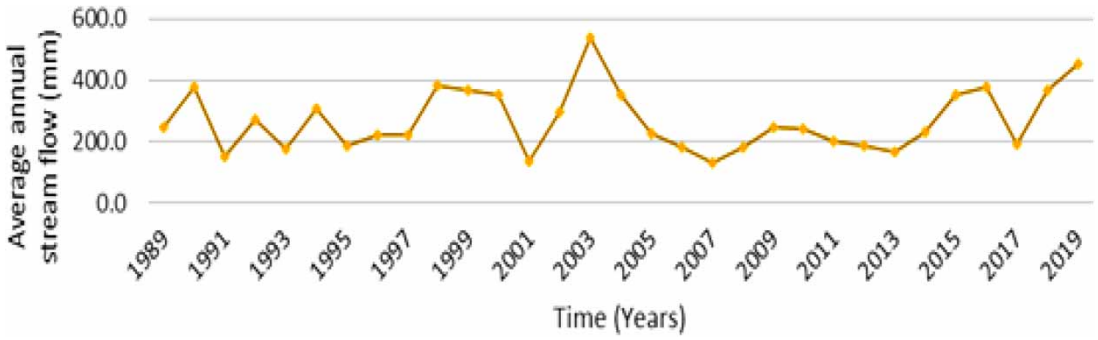

Figure 4 | The average annual streamflow trend for a period from 1989 to 2019.

Table 1 | Percentage variations in precipitation, temperature and stream flows

Period	Average *P* (mm)	Δ (%)	Average *T* (°C)	Δ (%)	Average *Q* (mm)	Δ (%)
1990–1999	1,035.93		15.7		267.7	
2000–2009	1,074.782	3.8	22.38	42.6	264.6	−1.2
2010–2019	1,181.732	10.0	22.16	−1.0	277.8	5.0

predetermined land use and land cover (LULC) types by creating polygons around representative sites. The pixels enclosed by these polygons were then used to derive spectral signatures for the respective land cover types recorded by the satellite images. The maximum likelihood classifier, which is based on the probability that a

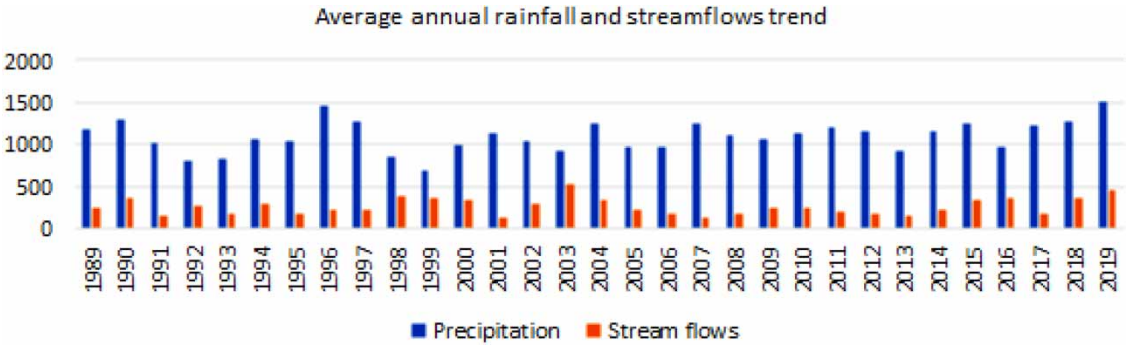

Figure 5 | Precipitation and stream flow variability.

pixel belongs to a particular class and takes the variability of classes into account by using the covariance matrix was used as the classification algorithm. Five classes were made out of the imagery and these were urban, barren lands, vegetation, open water and the stream.

A confusion matrix was then created using the ENVI software to give the overall accuracy, with the producer accuracies as well as the kappa coefficient. The overall accuracies and kappa coefficients were calculated based on Equations (2) and (3), respectively. LULC change analysis was then done by comparing the results obtained from three images.

$$\text{Overall accuracy} = \frac{\text{Total number of correctly classified pixels (diagonal)}}{\text{Total number of sample pixels}} \times 100 \tag{2}$$

$$\text{Kappa coefficient} = \frac{N\sum_{i=1}^{n} m_{i,i} - \sum_{i=1}^{n}(G_i C_i)}{N^2 - \sum_{i=1}^{n}(G_i C_i)} \tag{3}$$

where i is the class number; N is the total number of classified values compared to truth values; $m_{i,i}$ is the number of values belonging to the truth class i that have also been classified as class i (i.e. values found along the diagonal of the confusion matrix); C_i is the total number of predicted values belonging to class i; G_i is the total number of truth values belonging to class i

The methodology adopted in the prediction of future LULC is shown in Figure 6. The output LULC images for the years 1989, 2009 and 2019 shown in Figure 7(a)–7(c), respectively, were used to predict the future LULC image by using LCM of TerrSet. Shapefiles for the road network, rivers and urban centers for the Kyambura catchment were downloaded from the open street map at https://extract.bbbike.org/. A digital elevation map from SRTM Data was downloaded from the USGS Earth Explorer. Raster files for the distance from rivers, roads and urban centers were then developed using ArcGIS. These were then converted into ASCII format and fed to the LCM as prediction variables. The LCM was then run with land-cover maps of 1989 and 2009 as the initial and later land-cover maps of the catchment, respectively, to obtain a land-cover map of 2019. The LULC image of 2014 was predicted first and compared with the actual LULC image of 2014 developed in ArcMap. The model was then validated and 90% accuracy was obtained. Using LULC images of 2009 and 2019, the LULC image of 2050 shown in Figure 8 was predicted.

3.4. Design specifications of hydropower plant

The hydropower generation is a function of the flow discharge, head and density of water. The gross hydropower generation in watts can be calculated using the following equation.

$$E = \rho g Q \Delta h \eta \tag{4}$$

where ρ is the density of water, with $\rho = 10^3$ kg/m^3; g is the gravitational acceleration, with $g = 9.81$ m/s^2; Q is the flow discharge (m^3/s); Δh is the difference in elevations between the water level at the intake of the dam and the outlet of the turbine (m); and η is the efficiency of turbines (Li *et al.* (2018)). The design specifications for the

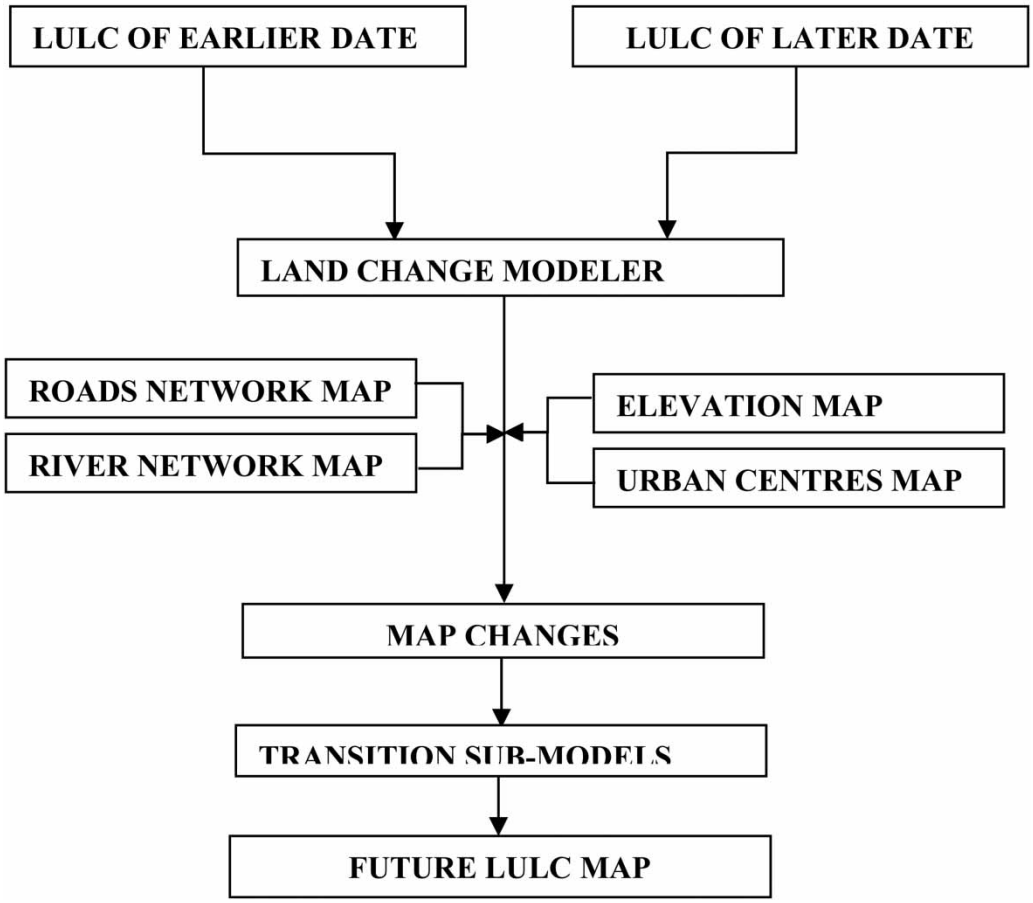

Figure 6 | LULC map prediction methodology.

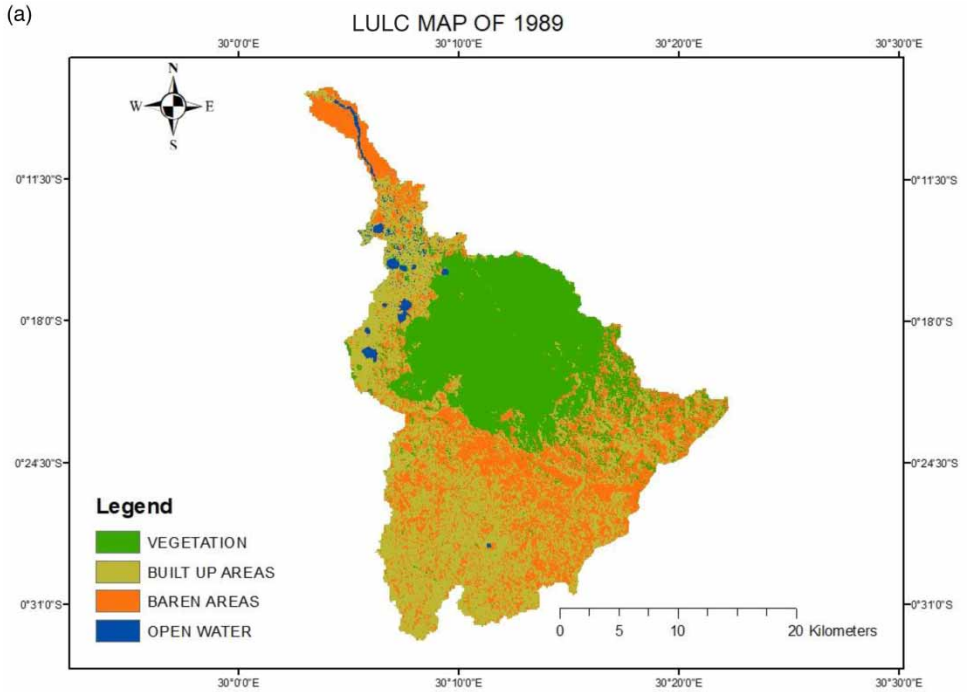

Figure 7 | (a) LULC map of 1989. (b) LULC map of 2009. (c) LULC map of 2019. (*continued*).

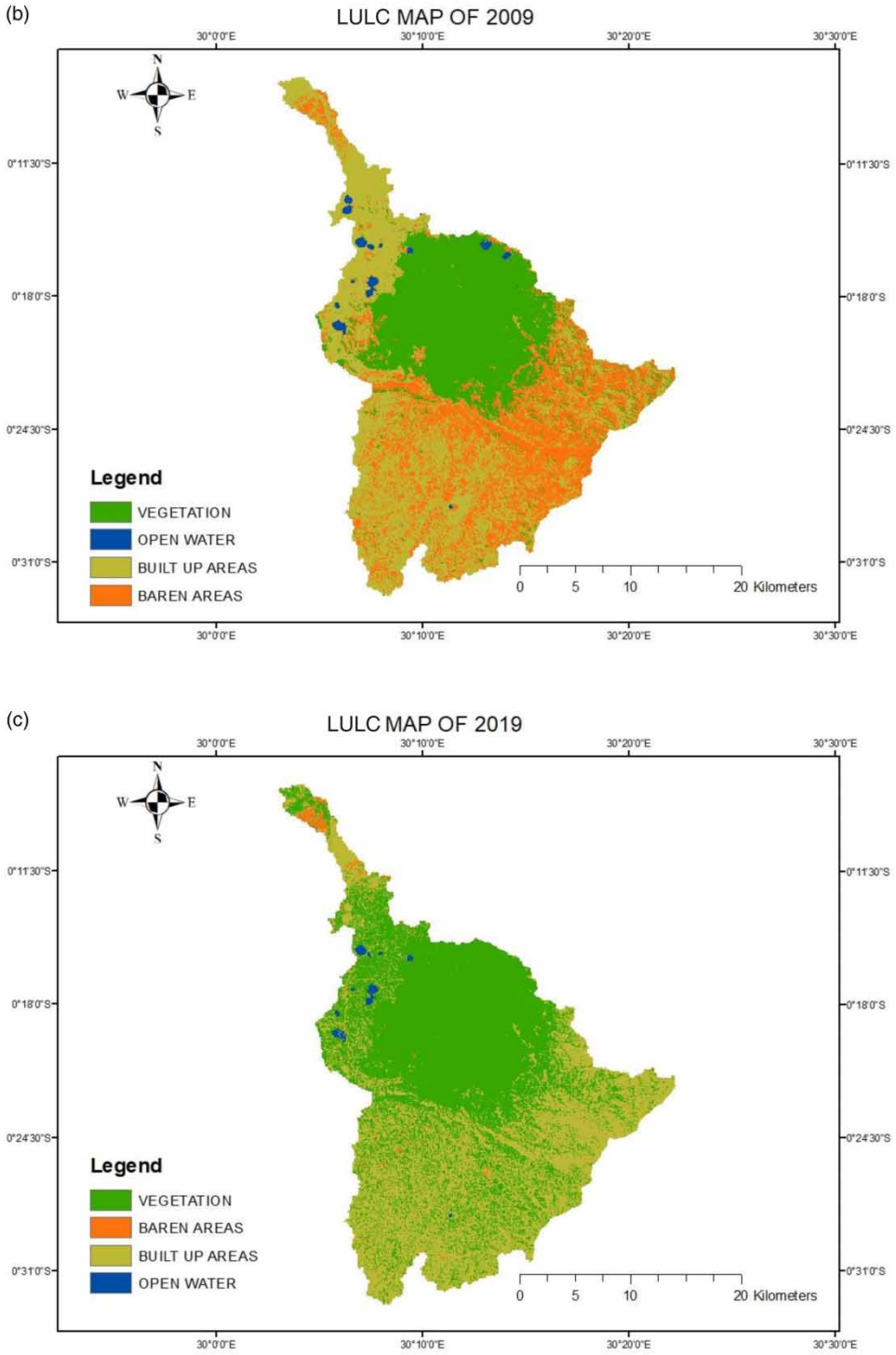

Figure 7 | Continued.

Kyambura small hydropower plant listed in Table 2 were obtained from the Ugandan Ministry of Energy, Oil and Mineral Development.

With a plant/capacity factor of 51%, the plant was designed to operate at almost half capacity. This implies that the plant's actual generation capacity is about 3,876 KW.

3.5. Model configuration

In the ArcSWAT, a project directory was set up to store all necessary folders and databases. The digital elevation model (DEM) was loaded from its folder on the disk as a Geographical Information System (GIS) layer into the

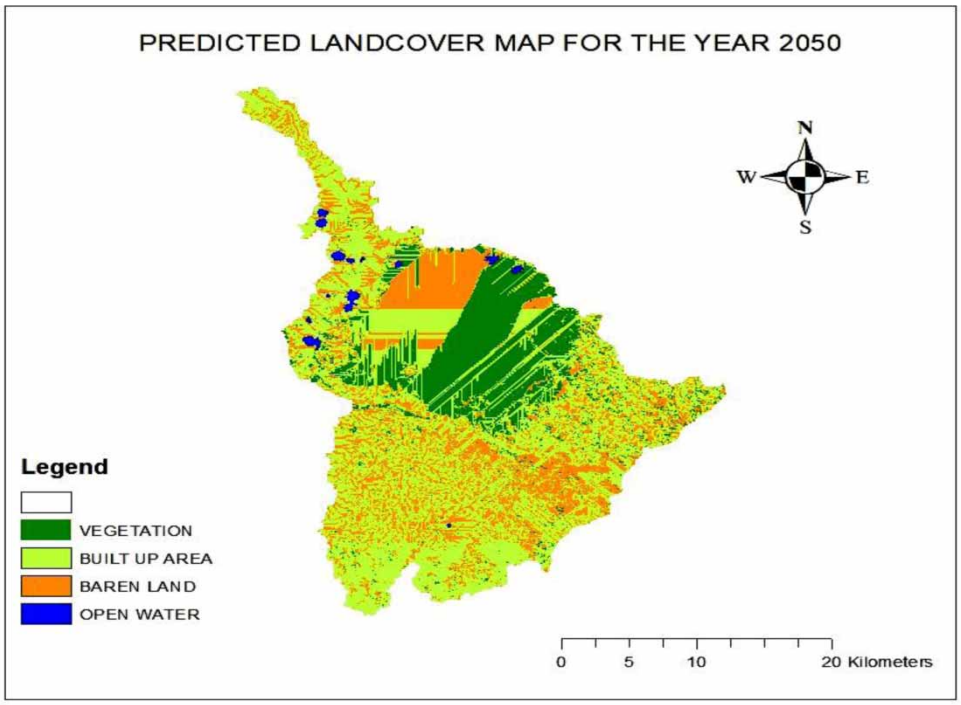

Figure 8 | LULC map of 2050.

Table 2 | Kyambura small hydropower plant design specifications

Technical specifications	
E	7,600 kW
Q	5 m^3/s
ΔH	102 m
Turbine	Francis
Generator	4,500 kva × 2
Plant factor	51%
Turbine efficiency	0.95

ArcSWAT project and its units for Z were set to meters. The watershed was then delineated using the Automatic Watershed Delineation tool found in the watershed delineator. The delineated Kyambura River watershed is as shown in Figure 9.

The definition of the stream network, outlet and inlet of the watershed was done using the threshold area method. The watershed was then divided into 29 hydrological response units (HRUs) which are areas with the same slope, soil type and land use. A map showing HRUs is shown in Figure 10.

The weather data were added and simulated from the global weather using the nearest gauge stations. This was done after all the geo-processing was done on DEM, land use and slope data. The Number of Years to SKIP (NYSKIP) variable was set to 3 to act as the warm-up period to process the data. The model was run to simulate the results at different periods. The model was then calibrated, evaluated and validated. The average annual water yield, which is a function of surface runoff, groundwater, lateral flow and transmission loss, was tabulated and plotted as shown in the following equation.

$$\mathrm{WYLD} = \mathrm{SR} + \mathrm{GF} + \mathrm{TF} - \mathrm{TL} \tag{5}$$

where WYLD is Water yield, SR is surface runoff, GF is groundwater flow, TF is tile flow and TL is transmission loss. Since water yield is a function of changes in land use/cover changes, two regression models were developed to define the relationship between the stream flows and water yield, and hydropower and water yield.

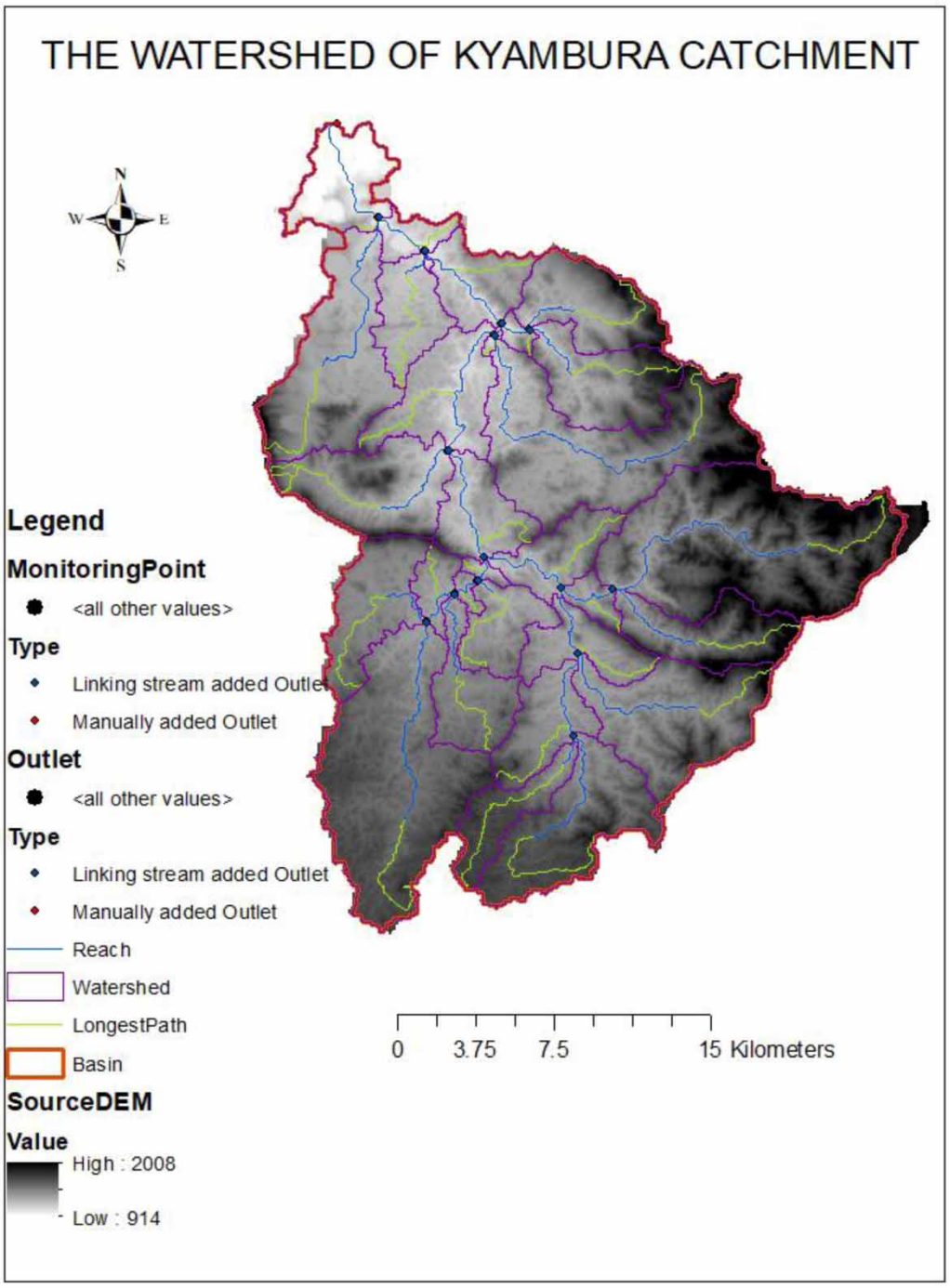

Figure 9 | Delineated River Kyambura Watershed.

3.6. Sensitivity analysis, calibration, and validation of the SWAT model

Prior to calibration, sensitivity analysis was executed for the control point to identify the most influential parameters. This also assisted in saving time throughout calibration since it minimized the number of parameters to be optimized in an over-parameterized SWAT model. The most sensitive parameters to stream flow were ALPHA_BF and CN2 at 0.05 level of significance. Based on the previous studies, the parameters that drive streamflow within the swat model were considered for calibration and validation. The monthly data for the years 2010–2013 were considered for Calibration. The model performance was then evaluated using the coefficient of correlation (R^2) as the objective function (Equation (6)). The model was then validated using monthly

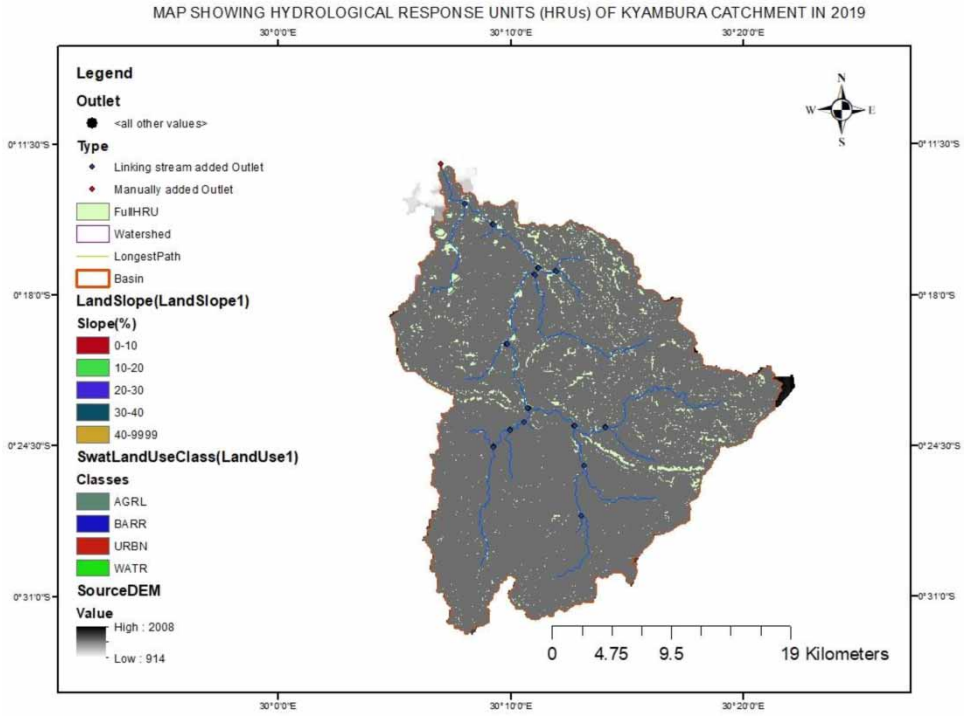

Figure 10 | Map showing the different HRUs of the Kyambura watershed.

data for the period of 2004–2006.

$$R^2 = \frac{\sum (Q_{obs} - \overline{Q_{obs}})^2 - \sum (Q_{sim} - \overline{Q_{sim}})^2}{\sum (Q_{obs} - \overline{Q_{obs}})^2} \quad (6)$$

where Q_{obs} is the observed discharge, Q_{sim} is the simulated discharge, $\overline{Q_{obs}}$ is the mean of observed discharge, and $\overline{Q_{sim}}$ is the mean of simulated discharge. R^2 indicates how the simulated data correlate to the observed values of data. The range of R^2 extends from 0 (unacceptable) to 1 (best) (Gebre 2015).

The top of the formula is the Residual sum of squared errors of the regression model (SSres). The bottom of the formula is the total sum of squared errors (SStot). This is comparing the actual y values to our baseline model the mean.

3.7. Climate change prediction

SDSM version 4.2 software was used to downscale meteorological data and perform climate predictions of the Kyambura Catchment for the year 2050. Daily mean temperature and precipitation obtained from the National Aeronautics and Space Administration (NASA) website were organized in Notepad ++ and saved in DAT format. ESM2 downscaling predictors for the study area were downloaded from https://climate-scenarios.Canada.ca. The SDSM settings were tailored to the precipitation prediction criteria. The data were then checked for any errors and discontinuity using the quality control panel. Predictor variables were then screened, set to NCEP-NCAR_1961_2005 and analyzed. The correlation coefficients for all variables were analyzed and four variables with P-values equal to zero or minimum and maximum correlation coefficients were recorded as shown in Table 3.

The four variables were also analyzed to obtain the best two predictor variables. The ncepmslpgl.dat and ncepp500gl.dat with correlation coefficients of −0.089 and 0.058 met the desired criteria and hence were used to predict the future precipitation of the Kyambura catchment. The model was then calibrated using the 'calibrate model' panel. The scenario generator was then used to generate precipitation data for the period of 2020–2100, 2020–2035 and 2043–2050. The predicted precipitation output file for the year 2050 was then compared with the 2019 calibrated precipitation data.

Table 3 | Predictor variables

Predictor variable	Partial *r*	*P*
ncepmslpgl.dat	−0.069	0.0000
ncepp500gl.dat	0.060	0.0000
ncepp8zhgl.dat	0.054	0.0000
Nceptempgl.dat	0.038	0.0002

Changes were then made in model settings to suit temperature analysis and prediction. The procedure above was then repeated for the temperature data file with ncepp8_ugl.dat and ncepp8_vgl.dat with the final correlation coefficients of 0.056 and 0.045, respectively, chosen as the most suitable predictor variables. The predicted temperature output file for the year 2050 was then compared with the 2019 calibrated temperature data.

3.8. Scenario analysis

The following scenarios were then created;

1. **KYA-SCEN 1:** In this scenario, the LULC map for the year 2019 was assumed to remain constant till 2050 and the climate was varied as predicted. Together with the LULC image of 2019, the predicted precipitation and temperature data were input into the calibrated and validated ArcSWAT model. The model was run and the monthly stream flow for the year 2050 was obtained.
2. **KYA-SCEN 2;** In this scenario, both LULC and climatic conditions were varied. The predicted LULC map, temperature and precipitation data for the year 2050 were input into the calibrated and validated ArcSWAT model. The model was run and the monthly stream flow for the year 2050 was obtained.

4. RESULTS AND DISCUSSION

4.1. Change analysis for LULC

From the error matrices developed, the accuracy of classification for each land use/land cover class for the different images of the different years was calculated. The overall accuracy of the classifications for each year with their Kappa coefficients is shown in Table 4.

Table 4 | LULC classification accuracy

Year	Overall accuracy	Kappa coefficient
2019	89.17	0.86
2009	96.67	0.96
1989	96.67	0.96

The results of the image classification as shown in Table 5 presented as percentage area coverage of each LULC class show a significant change in four land use types. The open water area reduced from 1.38% in 1989 to 0.51% in 2019 and is predicted to rise to 1.0% in 2050, Barren Land reduced from 26.95% in 1989 to 1.22% in 2019 and

Table 5 | Percentage areas per class for the different years

Year	1989	2009	2019	2050	% (1989–2009)	% (2009–2019)	% (2019–2050)
Vegetation	33.2	30.64	55.17	17.00	−2.6	24.5	−38.17
Built-up	38.47	39.61	43.11	55.00	1.1	3.5	11.89
Barren land	26.95	28.91	1.22	27.00	2.0	−27.7	25.78
Open water	1.38	0.84	0.51	1.00	−0.5	−0.3	0.49
Total	**100**	**100**	**100**	**100**			

is predicted to increase to 27% by 2050, Built-up area/Urban land increased from 38.47% in 1989 to 43.11% in 2019 and it is expected to further increase to 55.0% by 2050 whereas Vegetation area increased from 33.2% in 1989 to 55.17% in 2019 and it is predicted to tremendously reduce to 17.0% by 2050.

The reduction in the Barren land area for (the 1989–2019) period, is highly attributed to the large-scale commercial farming such as cotton and coffee farming within the watershed. Much of the redundant land has been turned into farmland hence an increase in vegetation area coverage. This has reduced the ability of the watershed to retain water in the soil. Consistent tillage of land increases the porosity of the soil, which results in an increased seepage rate and lateral flow of rainwater from the soil to the open water during wet seasons. It also increases the evaporation rate of moisture from the soil hence reducing the amount of water stored within the soil. By 2050, barren and urban land are expected to increase due to rural-urban migration, the infertility of soils to support agricultural work, and the rise in population. The increase in Built-up land creates more impervious surfaces where rainwater cannot seep into the soil. This leads to an increase in the runoff volume during rainy seasons that might even cause flooding in the watershed. Since little rainwater percolates into the soil, then very little water is stored within the watershed. This reduces the baseflow volume leading to low river flows during the dry seasons. The reduction in open water for the (1989–2019) period was due to the drying up of some streams within the catchment as well as weed growth on top of some crater lakes. This is expected to increase to 1% by 2050 if better open water management practices are implemented.

Other researchers (Alibuyog *et al.* 2009; Zhang *et al.* 2012; Anaba *et al.* 2017; Anand *et al.* 2018) have also found relatively similar LULC trends with their associated impacts in Murchison Bay Catchment, Ganga basin, Yangtze River basin and Manupali Sub-watershed, respectively.

4.2 Model simulations, calibration and validation

Model calibration was done by adjusting the most sensitive parameters such as R__CN2, V__ALPHA-BF, V__GW-DELAY and V__GWQMN to obtain the best fit between the model simulated stream flows and the observed/field streamflow data. Table 6 and Figure 11 show the most sensitive model parameters, their fitted values and the graphical representation of the calibrated model, respectively. Figure 12 shows a graphical representation of the validated ArcSWAT model.

Table 6 | Some of the most sensitive model parameters and their fitted values

S.N.	Parameter	Fitted value	Minimum value	Maximum value
1	R_CN2	19.075478	0	63.584923
2	V__ALPHA-BF	6.985367	−17.46342	17.463417
3	V__GW-DELAY	0.000031	−2,028.278	2,028.2783
4	V__GWQMN	0	−29,809.473	29,809.473

where R__CN2 is the moisture condition II of Initial SCS runoff curve number, V__ALPHA-BF is the baseflow recession constant, V__GW-DELAY is the delay time of groundwater, and V__GWQMN is the threshold depth of water in the shallow aquifer required for return flow to occur.

The sensitivity of ALPHA_BF indicated a quick response and movement of water to the groundwater recharge and it was due to the hilly nature of the watershed. The sensitivity of CN2 indicated the rapid changes in land use. The sensitivity of Manning's coefficient of roughness in the model indicated the significance of streamflow channel material in the watershed.

Coefficient of correlation (R^2) values of 0.788 and 0.688 were obtained during calibration and validation, respectively. Since the R^2 values for both calibration and validation were closer to one, then the model was a representative of the hydrological response of the watershed.

4.3. Climate change analysis

The predicted precipitation and temperature for the year 2050 were compared with that of 2019 as shown in Figures 13 and 14.

From the above analysis, there is likely to be an increase in the total annual rainfall by 93.7495 mm which is an equivalence of 7% increase by the year 2050. Temperature is likely to increase by 0.5 °C by the year 2050. Wet seasons (March to May and September to November) are likely to continue getting wetter whereas dry seasons

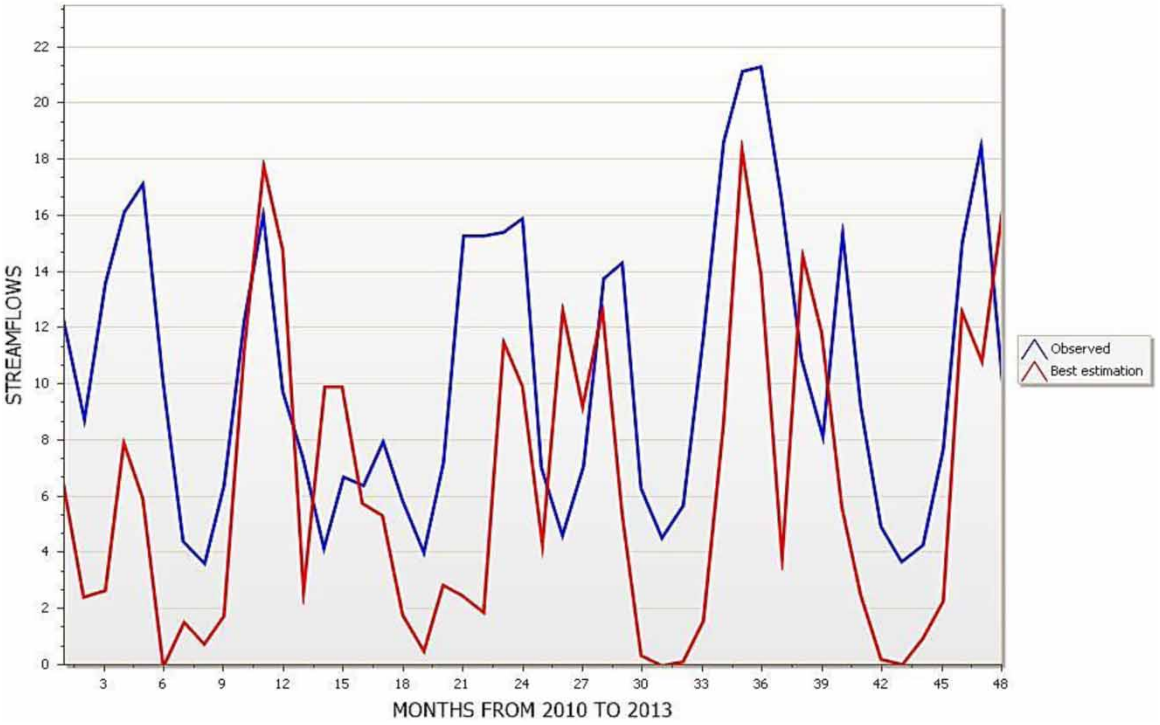

Figure 11 | The graphical representation of the calibrated model.

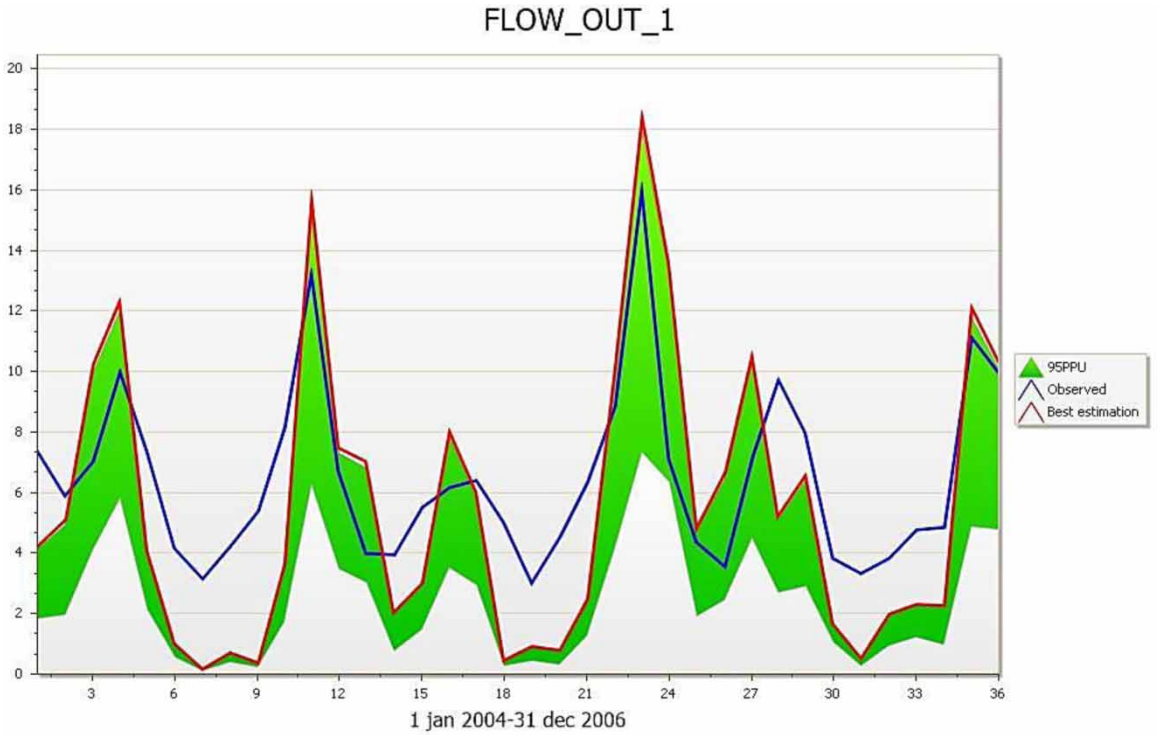

Figure 12 | The graphical representation of the validated model.

(December to February and June to July) are likely to continue getting drier. The observation agrees with Neema (2018) who indicated that the daily mean temperature and mean annual rainfall of Kyambura Watershed are likely to increase by 1.2 °C and 6%, respectively, by the year 2050. Similarly, Bahati *et al.* (2021) reported that

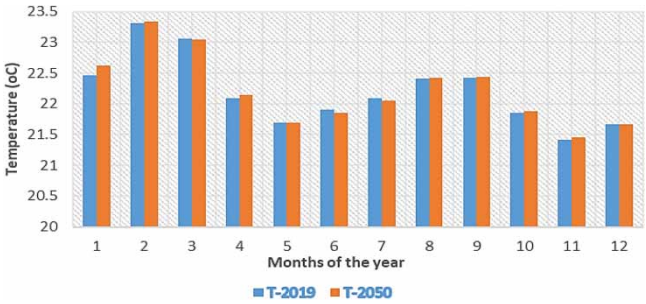

Figure 13 | Comparison between temperature for 2019 and predicted temperature for 2050.

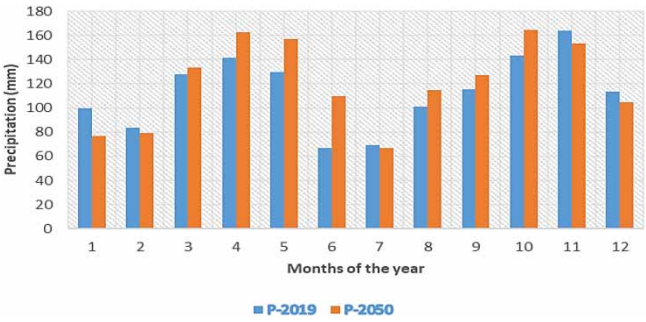

Figure 14 | Comparison between precipitation for 2019 and predicted precipitation for 2050.

there will be an increase in annual total rainfall by the percentage range of 2–10% as well as an increase in both annual minimum temperatures in the range of 0.8–2.5% and annual maximum temperatures in the range 0–0.4%.

4.4. Scenario analysis

4.4.1. KYA-SCEN 1

With the land-use assumed to remain constant and the climate changing, there is likely to be an increase in the mean annual streamflow of about 12%. Much rainfall will be experienced during the rainy seasons as shown in Figure 15.

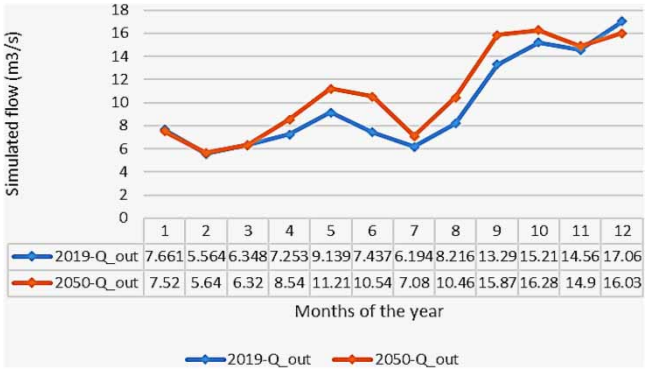

	1	2	3	4	5	6	7	8	9	10	11	12
2019-Q_out	7.661	5.564	6.348	7.253	9.139	7.437	6.194	8.216	13.29	15.21	14.56	17.06
2050-Q_out	7.52	5.64	6.32	8.54	11.21	10.54	7.08	10.46	15.87	16.28	14.9	16.03

Figure 15 | Comparison between simulated streamflow for the years 2019 and 2050.

4.4.2. KYA-SCEN 2

With both LULC and the environment changing, there is likely to be an increase in the mean annual streamflow by 18%. The wet seasons will continue getting wetter whereas dry seasons will continue getting drier as shown in Figures 16 and 17.

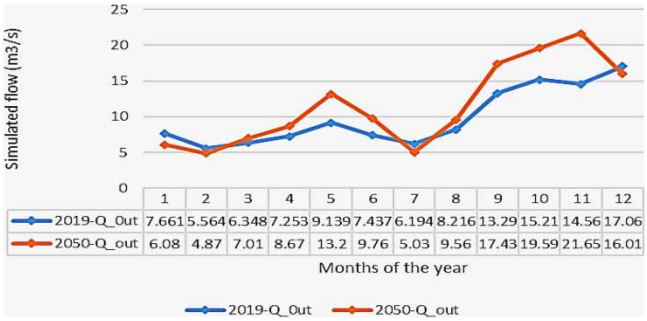

Figure 16 | Comparison between simulated streamflow for the years 2019 and 2050.

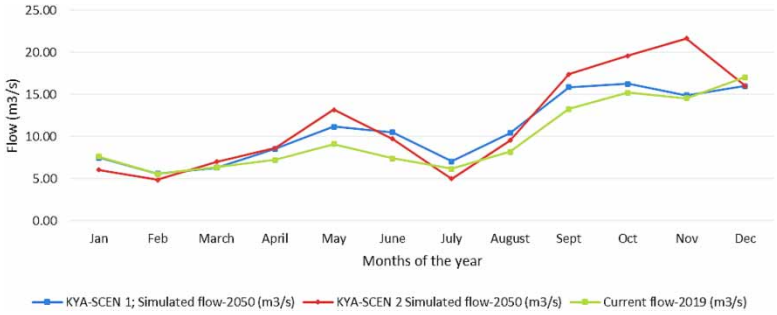

Figure 17 | Comparison between current stream flow and predicted simulated flow in 2050.

From the model output results and analysis, maximum and minimum streamflow was observed in the high and low rainfall months respectively. Streamflow was increased with the increasing rainfall and decreased with decreasing rainfall. The results also show that most of the rainfall was lost by evapotranspiration and very much less amount was lost through percolation. The groundwater flow of the watershed was very less in the watershed. The high concentration of groundwater flow contribution to the stream was due to high infiltration and much lower in vegetated areas due to the dominance of tile drainage. Unlike surface runoff, the lateral flow was higher in high infiltration regions and lower in flat land. The increase in built-up areas created more impermeable surfaces that affected the infiltration rate which led to reduced lateral flow. This resulted in very high surface runoff volumes during rainy seasons. Nie *et al.* (2011), Tang *et al.* (2005), and Maalim *et al.* (2013), also made similar observations that, an increase in urban set-up increases impervious surfaces and declining forest lands which results in accelerated surface runoff. This decreased lateral flow and groundwater recharge. In the long run, the river experienced high flows during rainy seasons which slowly dwindle with a scarcity of rain. This implies that stream flows vary with changes in land use/cover. The steady increase in streamflow is a result of good land management practices and leads to consistent flows across the year. Figure 18 shows the relationship between streamflow (Q), precipitation (P) and temperature (T) for the year 2050.

Figure 18 shows that an increase in rainfall results in an increase in streamflow. Zuo *et al.* (2016) suggest that changes in streamflow can be mostly attributed to changes in climate than changes in LULC. Whereas Yan *et al.* (2013) state that fluctuations in streamflow are due to changes in farmland, forests, and urban land, attribute it to both climate and land use changes. It can therefore be deduced that changes in streamflow for the Kyambura River are due to changes in both LULC and climatic conditions.

4.5. Hydropower generation response to climate and land use change analysis

The two study scenarios were showing a significant impact of climate and LULC change on the streamflow of river Kyambura.

By using the gross hydropower generation formula (Equation (4)), the average amount of power generated every month for the year 2019 and the two scenarios (KYA-SCEN 1 and KYA-SCEN 2), was calculated and plotted as shown in Table 7 and Figure 19.

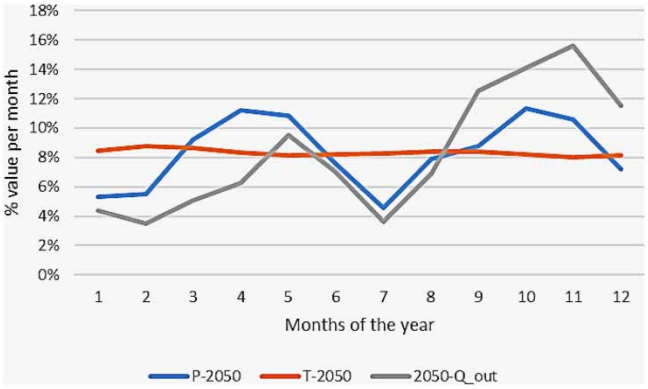

Figure 18 | Monthly percentage values of the predicted temperature (*T*), precipitation (*P*) and stream flow (*Q*).

Table 7 | Hydropower generated for the current and future streamflow

Month of the year	Current power (KW)	KYA-SCEN 1 power (KW)	Percentage change (%)	KYA-SCEN 2 power (KW)	Percentage change (%)
January	7,282.7	7,148.4	−1.8	5,779.6	−20.6
February	5,289.3	5,361.3	1.4	4,629.4	−12.5
March	6,034.7	6,007.7	−0.4	6,663.6	10.4
April	6,894.9	8,118.0	17.7	8,241.6	19.5
May	8,687.2	10,656.1	22.7	12,547.8	44.4
June	7,069.2	10,019.2	41.7	9,277.7	31.2
July	5,887.5	6,730.2	14.3	4,781.5	−18.8
August	7,810.2	9,943.2	27.3	9,087.6	16.4
September	12,636.5	15,085.8	19.4	16,568.8	31.1
October	14,461.2	15,475.6	7.0	18,622.0	28.8
November	13,843.7	14,163.8	2.3	20,580.3	48.7
December	16,215.2	15,237.9	−6.0	15,218.9	−6.1

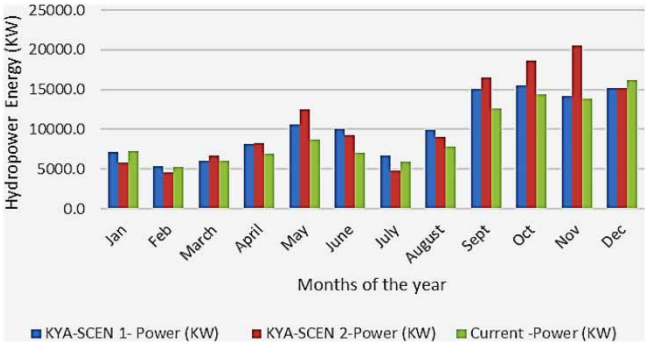

Figure 19 | The potential change in hydropower generation.

The graphical analysis in Figure 19 shows a general increase in hydropower generation within Kyambura Catchment if land use changes are controlled. For scenario KYA-SCEN 1, the maximum mean monthly power of 15,237.9 KW was obtained in the month of December and the least mean monthly power of 5,361.3 KW in the month of February. For Scenario A2, the maximum mean monthly power of 20,580.3 KW and the least mean monthly power of 4,629.4 KW in the months of November and February, respectively. In comparison with the present/current power potential, there will be a general increase in the amount of power produced in

2050. The total annual power generated was predicted to increase by 10.6 and 17.7% for KYA-SCEN 1 and KYA-SCEN 2 scenarios, respectively. These observations agree with Bahati *et al.* (2021) who found that the mean annual discharges for Muzizi River will be more than the designed discharges in the future. The mean annual hydropower is therefore expected to rise significantly above the design capacity of the power station.

The analysis further shows that high power loads will be generated during wet seasons (March to May and September to November) and very low in dry seasons (December to February and June to July). During the two dry seasons, the amount of power generated goes below the 7,600 KW design capacity in February and July whereas during the wet seasons, it goes above the design capacity. This may cause load-shedding during dry seasons and hence slows down economic development within the Kyambura watershed. Since hydropower is a function of flow discharge, head and the density of water. Any changes in the flow, pressure head and hydrological properties of the watershed will affect the amount of power generated.

In the river Kyambura watershed, land use and land cover changes have had and are still having an impact on the flow regime of the river through the variation of the streamflow. Changes in streamflow result in fluctuating power.

The observation above indicates that low streamflow, which is a result of poor land management practices and changes in climatic conditions, results in low power output due to low river flows. Low and high streamflow are experienced in dry and wet seasons, respectively. This can be attributed to the failure of the watershed to easily allow water to percolate into the soil and store it for consistent lateral flow. The shallow aquifers within the watershed are not adequately recharged to keep the river's flow consistent. Therefore, for the Kyambura hydropower station to operate at its required capacity throughout the year, better land management practices should be implemented to improve the integrity of the watershed. Climate change should also be averted through better practices such as afforestation, reduction of carbon emissions, afforestation among others.

5. CONCLUSIONS AND RECOMMENDATIONS

5.1. Conclusions

Similar to the conclusions of Duong *et al.* (2016) and Bahati *et al.* (2021), this study has shown that changes in climate and land use/cover have an impact on hydropower generation in the Kyambura catchment. Land use image classification results show a change in land use and land cover within the Kyambura catchment. The open water area reduced from 1.38% in 1989 to 0.51% in 2019 and was predicted to rise to 1.0% in 2050, Barren land reduced from 26.95% in 1989 to 1.22% in 2019 and was predicted to increase to 27% by 2050, Built-up area/Urban land increased from 38.47% in 1989 to 43.11% in 2019 and it was expected to further increase to 55.0% by 2050 whereas Vegetation area increased from 33.2% in 1989 to 55.17% in 2019 and it was predicted to tremendously reduce to 17.0% by 2050. The classification was performed with an accuracy range of 89.17–96.67% and a corresponding kappa coefficient range of 0.86–0.96. Land use changes were found to affect the streamflow of river Kyambura.

Correlation coefficients (R^2) of 0.788 and 0.688 were obtained during ArcSWAT model calibration and validation, respectively. From the climate prediction and analysis, the total annual rainfall was predicted to increase by 93.7495 mm which is an equivalence of 7% increase by the year 2050. Temperature predictions gave a 0.5 °C increase by the year 2050.

Study scenarios KYA-SCEN 1 and KYA-SCEN 2 showed an increase in streamflow by 12 and 18%, respectively. Due to the increase in simulated flows, computations show that there will be a 10.6 and 17.7% increase in average annual hydropower generated by the Kyambura mini-hydropower station by the year 2050.

The study therefore reveals that there is a strong relationship between climate, LULC change, stream flows and eventually hydropower generation.

5.2. Recommendations

The aim of this study was to contribute knowledge to hydropower and engineering professionals on the impacts of land use and climate change on hydropower reliability in the development of hydropower stations on small rivers. Whereas this has been demonstrated, it should be noted that the analysis is limited to the hydrological dimension and has not considered aspects such as sedimentation. Given that the changes in the predicted hydropower potential are due to changes in streamflow caused by changes in climate and LULC, the risk of sedimentation on mini-hydropower stations such as the Kyambura small-hydropower station cannot be ruled out. It is therefore recommended that National Environmental Management Authority (NEMA) develops a

catchment-based environmental protection program through re-afforestation and enforcing buffer zones alongside the Kyambura River.

Governing policies such as one that governs operations and land management practices in such hydropower generation catchments will also help to preserve the integrity of the watersheds. This study did not consider the impacts of sedimentation on the hydropower station. It is therefore recommended that future studies be carried out in this regard.

ACKNOWLEDGEMENTS

This work reported here was undertaken as part of *Building Capacity in Water Engineering for Addressing Sustainable Development Goals in East Africa (CAWESDEA)* which is part of the IDRC-funded programme on Strengthening Engineering Ecosystems in sub-Saharan Africa. The CAWESDEA Project is led by Global Water Partnership Tanzania in collaboration with Makerere University (Uganda), Moi University (Kenya) and the University of Dar es Salaam (Tanzania).

DATA AVAILABILITY STATEMENT

All relevant data are included in the paper or its Supplementary Information.

CONFLICT OF INTEREST

The authors declare there is no conflict.

REFERENCES

Abbaspour, K. 2007 *User Manual for SWAT-CUP, SWAT Calibration and Uncertainty Analysis Programs*. Swis Federal Institute of Aquatic Science and Technology, Switzerland.

Alibuyog, N., Ella, V., Reyes, M., Srinivasan, R., Heatwole, C. & Dillaha, T. 2009 Predicting the effects of land use change on runoff and sediment yield in Manupali river subwatersheds using the SWAT model. *International Agricultural Engineering Journal* **18**, p. 15.

Amanyire, S. 2019 *Urban River Pollution: A Case Study of River Mpanga in Fortportal City*, Kabarole District. Makerere University

Amini, A., Ali, T. M., Ghazali, A. H. B., Aziz, A. A. & Akib, S. M. 2011 Impacts of Land-Use Change on Streamflows in the Damansara Watershed, Malaysia. *Arab J Sci Eng* **36**, 713–720. https://doi.org/10.1007/s13369-011-0075-3

Anaba, L., Banadda, N., Kiggundu, N., Wanyama, J., Engel, B. & Moriasi, D. 2017 Application of SWAT to assess the effects of land use change in the Murchison Bay catchment in Uganda. *Computational Water, Energy, and Environmental Engineering* **6**, 24–40. doi:10.4236/cweee.2017.61003.

Anand, J., Gosain, A. K. & Khosa, R. 2018 Prediction of land use changes based on land change modeler and attribution of changes in the water balance of Ganga basin to land use change using the SWAT model. *Science of The Total Environment* **644**, 503–519. doi: 10.1016/j.scitotenv.2018.07.017.

Arnold, J. G., Srinivasan, R., Muttiah, R. S. & Williams, J. R. 1998 Large area hydrologic modeling and assessment part I: model development 1. *JAWRA Journal of the American Water Resources Association* **34**(1), pp. 73–89.

Bahati, H. K., Ogenrwoth, A. & Sempewo, J. I. 2021 Quantifying the potential impacts of land-use and climate change on hydropower reliability of Muzizi hydropower plant, Uganda. *Journal of Water and Climate Change* jwc2021273. https://doi.org/10.2166/wcc.2021.273.

Bartle, A. 2002 Hydropower potential and development activities. *Energy Policy* **30**, 1231–1239.

Bosmans, J. H. C., Beek, L. P. H. R. V., Sutanudjaja, E. H. & Bierkens, M. F. P. 2016 Hydrological impacts of global land cover change and human water use. 1–31. https://doi.org/10.5194/hess-2016-621.

Bu, H., Meng, W., Zhang, Y. & Wan, J. 2014 Relationships between land use patterns and water quality in the Taizi River basin, China, *Ecological Indicators* **41**, 187–197, ISSN 1470-160X, https://doi.org/10.1016/j.ecolind.2014.02.003.

Calder, T. 1998 *Water Resource and Land-Use Issues*. Water management Institute, Colombo, Sri Lanka. Available from: http://www.cgiar.org/iwmi/pubs/swimpubs/Swim03.pdf

Cole, M. A., Elliott, R. J. R. & Strobl, E. 2014 Climate change, hydro-dependency, and the African Dam Boom. *World Development* **60**, 84–98. https://doi.org/10.1016/j.worlddev.2014.03.016.

Core Writing Team, Pachauri, R. K. & Meyer, L. A. & IPCC Climate Change 2014 *Synthesis Report Summary for Policymakers. Contribution of Working Groups I, II and III to the Fifth Assessment Report of the Intergovernmental Panel on Climate Change*. IPCC, Geneva, Switzerland.

Di Luzio, M. R. S. 2001 *ArcView Interface for SWAT 2000*.

Duong, P. C., Naudit, A., Nam, D. H. & Phong, N. T. 2016 *Assessment of Climate Change Impacts on River Flow Regimes in the Red River Delta, Vitenam-A Case Study of the Nhue-Day River Basin*.

Fengping, L., Guangxin, Z. & Liqin, D. 2013 Studies for impact of climate change on hydrology and water resources. *Scientia Geographica Sinica* **33**(4), 457–464.

Gaudard, L., Gilli, M. & Romerio, F. 2013 Climate change impacts on hydropower management. *Water Resource Management* **27**, 5143–5156. https://doi.org/10.1007/s11269-013-0458-1.

Gaudard, L., Romerio, F., Valle, F. D., Gorret, R., Maran, S., Ravazzani, G., Stoffel, M. & Volonterio, M. 2014 Climate change impacts on hydropower in the Swiss and Italian Alps. *Science of The Total Environment* **493**, 1211–1221, ISSN 0048-9697, https://doi.org/10.1016/j.scitotenv.2013.10.012.

Gebre, S. L. 2015 Application of the HEC-HMS model for runoff simulation of Upper Blue Nile River Basin. *Journal of Waste Water Treatment & Analysis* **06**(02). doi:10.4172/2157-7587.1000199.

Guzha, A. C., Rufino, M. C., Okoth, S., Jacobs, S. & Nóbrega, R. L. B. 2018 Impacts of land use and land cover change on surface runoff, discharge and low flows: Evidence from East Africa, *Journal of Hydrology: Regional Studies* **15**, 49–67, ISSN 2214-5818, https://doi.org/10.1016/j.ejrh.2017.11.005.

Hamududu, B. & Killingtveit, A. A. 2012 Assessing climate change impacts on global hydropower. *Energies* **5**(2), 305–322. https://doi.org/10.3390/

Houghton, J. T., Ding, Y., Griggs, D. J., Noguer, M., van der Linden, P. J., Dai, X., Maskell, K. & Johnson, C. A. 2001 *Climate Change 2001: The Scientific Basis*. Cambridge University Press, Cambridge. https://doi.org/10.1002/hyp.7156

Kangume, C. 2016 *Assessing the Impact of Climate Change on Stream Flow in Malaba River*.

Kees, M. & Steven, v. E. (RVO.nl) 2018 'Final Energy report Uganda', Ministry of foreign affairs, Version 6.

Khare, D., Patra, D., Mondal, A. & Kundu, S. 2017 Impact of landuse/land cover change on run-off in the catchment of a hydro power project. *Applied Water Science* **7**(2), 787–800. https://doi.org/10.1007/s13201-015-0292-0.

Labat, D., Godderis, Y., Probst, J. L. & Guyot, J. L. 2004 Evidence for global runoff increase related to climate warming. *Advances in Water Resources* **27**(6), 631–642.

Li, J., Ameen, A. M. S., Mohammad, T. A., Al-Ansari, N. & Yaseen, Z. M. 2018 A systematic operation program of a hydropower plant based on minimizing the principal stress: Haditha Dam case study. *Water* **10**(9), 1270.

Liu, J., Kuang, W., Zhang, Z., Xu, X., Qin, Y., Ning, J., Zhou, W., Zhang, S., Li, R., Yan, C., Wu, S., Shi, X., Jiang, N., Yu, D., Pan, X. & Chi, W. 2014 Spatiotemporal characteristics, patterns, and causes of land-use changes in China since the late 1980s. *Journal of Geographical Sciences* **24**(2), 195–210.

Maalim, F. K., Melesse, A. M., Belmont, P. & Gran, K. B. 2013 Modeling the impact of land Use changes on runoff and sediment yield in the Le Sueur Watershed, Minnesota using GeoWEPP. *Catena* **107**, 35–45. https://doi.org/10.1016/j.catena.2013.03.004.

Madani, K. 2011 Hydropower licensing and climate change: insights from cooperative game theory. *Advances in Water Resources* **34**(2), 174–183. https://doi.org/10.1016/j.advwatres.2010.10.003.

Melih Ozturk, N. K. 2013 Modeling the impact of land use change on the hydrology of a rural watershed. (C. Corradini, Ed.). *Journal of Hydrology* **497**, 97–109.

Memarian, H., Tajbakhsh, M. & Balasundram, S. K. 2013 Application of swat for impact assessment of land use/cover change and best management practices: a review. *International Journal of Advancement in Earth and Environmental Sciences* **1**(1), 36–40.

Musa, A. T. & Eliot, R. 2018 *Assessing the Effect of Land-Use Changes on the Flow Regime of River Rwizi*. Makerere University, Civil and Environmental Engineering, Kampala.

Neema, J. A. 2018 *Assessing the Effects of Climate Change on Stream Flow of River Kyambura*. Makerere University, Civil and Environmental Engineering, Kampala.

Neitsch, S. L., Arnold, J. G., Kiniry, J. R. & Williams, J. R. 2011 *Soil and Water Assessment Tool Theoretical Documentation Version 2009*. Texas Water Resources Institute.

Nie, W., Yuan, Y., Kepner, W., Nash, M. S., Jackson, M. & Erickson, C. 2011 Assessing impacts of landuse and landcover changes on hydrology for the Upper San Pedro Watershed. *Journal of Hydrology* **407**, 105–114. https://doi.org/10.1016/j.jhydrol.2011.07.012.

Ogiramoi, P. 2011 *Climate Change Impacts on Hydrological Extremes and Water Resources in Lake Victoria Catchments, Upper Nile Basin*. Department of Civil Engineering, Katholieke Universiteit Leuven Kasteelpark Arenberg 40, 3001 Heverlee, Belgium.

Pachauri, R. K., Allen, M. R., Barros, V. R., Broome, J., Cramer, W., Christ, R., Dubash, N. K., 2014 Climate change 2014: synthesis report. In: *Contribution of Working Groups I, II and III to the Fifth Assessment Report of the Intergovernmental Panel on Climate Change* (Pachauri, R. & Meyer, L., eds). IPCC, Geneva, Switzerland, pp. 151.

Renewgen 2021 *'Kyambura Small Hydro Power Project'*. Renewgen.lk, Colombo, Sri Lanka. Retrieved 8 April 2021

Ronald Eastman, J. 1987–2016 *TerrSet Geospatial Monitoring and Modeling System Manual*., Clark Labs, Clark University, Worcester, Massachusetts.

Rugumayo, A., Taylor, T., Markandya, A. & Droogers, P. 2014 Economic assessment of the impacts of climate change in Uganda. *Costume* **8**(1), 61. https://doi.org/10.1179/cos. 1974.8.1.61.

Serrão, E. A. d. O., Silva, M. T., Ferreira, T. R., da Silva, V. d. P. R., de Sousa, F. d. S., de Lima, A. M. M., de Ataide, L. C. P., Thiago, R. & Wanzeler, S. 2020 Land use change scenarios and their effects on hydropower energy in the Amazon, *Science of The Total Environment*, **744**, 140981, ISSN 0048-9697,https://doi.org/10.1016/j.scitotenv.2020.140981

Sundara Kumar, K., Udaya Bhaskar, P. & Padmakumari, K. 2015 Application of land change modeler for prediction of future land use land cover; A case study of Vijayawada city. Department of Civil Engineering, University of Delhi (DU). 2nd International Conference on Science, Technology and Management.

Tang, Z., Engel, B. A., Pijanowski, B. C. & Lim, K. J. 2005 Forecasting land use change and its environmental impact at a watershed scale. *Journal of Environmental Management* **76**, 35–45. https://doi.org/10.1016/j.jenvman.2005.01.006.

Taye, M. T., Willems, P. & Block, P. 2015 Implications of climate change on hydrological extremes in the Blue Nile basin: a review. *Journal of Hydrology: Regional Studies* **4**, 280–293. https://doi:10.1016/j.ejrh.2015.07.001.

Taylor, T., Markandya, A., Droogers, P., Rugumayo, A. & Beucher, O. 2014 *Economic Assessment of the Impacts of Climate Change in Uganda Data Water Sector Report*.

Taylor, T., Markandya, A., Mwebaze, T., Sebbit, A. & Rautenbach, H. 2015 *Economic Assessment of the Impacts of Climate Change in Uganda; A Case Study on Water and Energy Sector Impacts in the Mpanga River Catchment* (Metro economical).

Tilak, H. 2010 Effect of land use in the upper Mahaweli catchment area on erosion, landslides and siltation in hydropower reservoirs of Sri Lanka. *Journal of the National Science Foundation of Sri Lanka* **38**, 1.

Uganda Bureau of Statics 2016 *Uganda National Household Survey 2016/2017*.

Welde, K. & Gebremariam, B. 2017 Effect of land use land cover dynamics on hydrological response of watershed: case study of Tekeze Dam watershed, northern Ethiopia. *International Soil and Water Conservation Research* **5**(1), 1–16. doi:10.1016/j.iswcr.2017.03.002.

Wilby, R. L. & Dawson, C. W. 2007 *SDSM 4.2 – A Decision Support Tool for the Assessment of Regional Climate Change Impacts*.

Wilby, R. L., Dawson, C. W. & Barrow, E. M. 2002 SDSM – a decision support tool for the assessment of regional climate change impacts. *Environmental and Modelling Software* **17**(2), pp. 145–157.

Winchell, M., Srinivasan, R., Di Luzio, M. & Arnold, J. 2010 *ArcSWAT Interface for SWAT2009 User's guide*. Temple, Texas: Blackland research and extension center.

Yan, B., Fang, N. F., Zhang, P. C. & Shi, Z. H. 2013 Impacts of land use change on watershed streamflow and sediment yield: an assessment using hydrologic modelling and partial least squares regression. *Journal of Hydrology* **484**, 26–37. https://doi.10.1016/j.jhydrol.2013.01.008.

Zhang, Z., Duan, J., Wang, S., Luo, C., Chang, X., Zhu, X., Xu, B. & Wang, W. 2012 Effects of land use and management on ecosystem respiration in alpine meadow on the Tibetan plateau. *Soil and Tillage Research* **124**, 161–169. ISSN 0167-1987, https://doi.org/10.1016/j.still.2012.05.012.

Zuo, D., Xu, Z., Yao, W., Jin, S., Xiao, P. & Ran, D. 2016 Assessing the effects of changes in land use and climate on runoff and sediment yields from a watershed in the loess plateau of China. *Science of the Total Environment* **544**, 238–250. https://doi.org/10.1016/j.scitotenv.2015.11.060.

First received 10 November 2021; accepted in revised form 4 May 2023. Available online 17 May 2023